Journal of Applied Polymer Science

Stille cross-coupling applied to get higher molecular weight polymers: Synthesis, optoelectronic, V_{oc} properties, and solar cell application

Muddasir Hanif, Linlin Chen, Li Zhu, Dan Zhao, Tianrou Xiong, Haoqing Hou

Department of Chemistry and Chemical Engineering, Jiangxi Normal University, Nanchang, Jiangxi 330022, People's Republic of China

Correspondence to: M. Hanif (E-mail: muddasirhanif@yahoo.com or hanif@jxnu.edu.cn) and H. Hou (E-mail: haoqing@jxnu.edu.cn)

ABSTRACT: Conjugated polymers are highly desirable for the photovoltaic applications. We report the synthesis, characterization, optoelectronic properties, and solar cell application of two polymers, namely, *poly*[(9,9-didodecylfluorene-2,7-diyl)-*alt*-(2,2′:5′,2″-terthiophene-5,5″-diyl)] (P1) and *poly*[(1,4-bis(dodecyloxy)benzene-2,5-diyl)-*alt*-(2,2′:5′,2″-terthiophene-5,5″-diyl)] (P2). The polymers were synthesized via Stille cross-coupling reaction, and were characterized by the gel permeation chromatography, nuclear magnetic resonance, Fourier transform infrared, UV–vis, thermogravimetric analysis, and cyclic voltammetry analyses. The two copolymers are processable due to their good solubility in organic solvents (tetrahydrofuran, $CHCl_3$, toluene, chlorobenzene, and *o*-dichlorobenzene). The optical band gaps (UV–vis, film, and E_g^{opt}) of the P1 and P2 are 2.04 and 2.00 eV, respectively. The density functional theory output structures showed that S···O space interaction is likely responsible for the higher planarity of P2. The polymers showed low HOMO energy levels (P1: −5.33 eV, P2: −5.05 eV). The E_{HOMO} for P1 is close to the E_{HOMO} (−5.4 eV) of an ideal polymer, which is an important, rare, and main origin of the observed higher V_{oc} (801–808 mV). The onset decomposition temperatures (T_d) for the P1 and P2 are 418°C and 365°C, respectively. The polymer solar cell based on the P1: C_{60} (1: 1) and P2: C_{60} (1: 1) blend showed a power conversion efficiency (PCE) of 0.94 and 0.71%, respectively. The composite polymer : $PC_{60}BM$ = 1 : 2 increased PCE of the P1 (1.65%) and P2 (1.09%) under AM 1.5 illumination (100 mW/cm^2). The study provided important examples to design donor–donor (D–D) polymers for the photovoltaic applications. © 2015 Wiley Periodicals, Inc. J. Appl. Polym. Sci. **2015**, *132*, 42147.

KEYWORDS: copolymers; electrochemistry; optical and photovoltaic applications; synthesis and processing

Received 17 October 2014; accepted 23 February 2015

DOI: 10.1002/app.42147

INTRODUCTION

Solar cells based on organic conjugated polymers are attractive due to the low cost, light weight, flexibility, and solution processability.[1–3] A bulk heterojunction (BHJ) polymer solar cell (BHJ-PSCs) uses conjugated polymers as the electron donor and fullerene or fullerene derivative as the electron acceptor for the photo-induced charge generation and transport in the BHJ-solar cells, with power conversion efficiency (PCE) range of 0.04–8%.[4–7] An ideal polymer for the organic photovoltaic (OPV) application should have the properties such as high absorption, small band gap (1.5 eV), thermal stability, high charge carrier mobility (10 cm^2 V^{-1} s^{-1}), π-stacking, good molecular weights, good film-forming properties, and suitable energy levels (E_{HOMO} = −5.4 eV, E_{LUMO} = −3.9 eV) with respect to the $PC_{60}BM$ (*n*-type materials).[8,9]

Generally conjugated polymers used for the BHJ-PSCs are of two main types: the first type contains same or different donor units or simply D–D polymers and the second type contains the donor and acceptor units or simply D–A polymers. The D–D polymers have the advantage of simpler synthesis and molecular structure which is an important factor for their mass production. Regio-regular *poly*(3-hexylthiophene-2,5-diyl) (*rr*-P3HT) is the best successful example of a D–D conjugated polymer. It has been reported for the *rr*-P3HT that the polymers with number average molecular weight, $M_n > 10$ kDa can show higher photo conversion efficiency (PCE = 2–3%) when compared to the lower $M_n = 2.2$ kDa (PCE ∼ 0.5%) under optimized conditions.[10]

Poly(fluorene-*alt*-thiophene) (PFTH, D–D polymer) are getting increasing research interest for example; Alex Adronov and coworkers have shown that single-walled carbon nanotubes (SWNTs, *n*-type material) and PFTH can form strong supramolecular complexes (PFTH-SWNT), leading to an excellent solubility, solution stability of complexes, and easier processing.[11] In 2007, Chen and coworkers reported the *poly*[(9,9-

Additional Supporting Information may be found in the online version of this article.

dihexylfluorene-2,7-diyl)-*alt*-(2,2′:5′,2″-terthiophene-5,5″-diyl)] (by Suzuki cross-coupling reaction: SzCCR) for the OFET application.[12] They found a number average molecular weight $M_n = 4720$ (PDI = 1.31), and HOMO energy level, $E_{HOMO} = -5.08$ eV. In 2012, Koehler and coworkers reported exactly the same polymer (named as LaPPs45) for the OPV application and found a highest V_{oc} of 0.68 V (680 mV) and highest solar cell efficiency $\eta = 2.33\%$ after optimization.[13] In 2013, Akcelrud and coworkers reported exactly the same polymer (LaPPs45, by SzCCR) for the OPV application.[14] They found $M_n = 2500$ (PDI = 2.2), $E_{HOMO} = -5.2$ eV, highest V_{oc} of 0.68 V (680 mV) and optimized $\eta = 2.33\%$. They also reported that the higher thiophene content in the polymer main chain is responsible for the sooner precipitation, interruption of the chain growth, lower M_n, and higher PDI of the polymer. To solve these problems, we increased the chain length on the C_9 of fluorene, kept the terthiophene same, and replaced the Suzuki cross-coupling with the Stille cross-coupling reaction to avoid the aqueous reagent (K_2CO_3) to have better solubility during polymerization. We have synthesized the *poly*[(9,9-didodecylfluorene-2,7-diyl)-*alt*-(2,2′:5′,2″-terthiophene-5,5″-diyl)] (P1) using above modifications which resulted in a higher molecular weight ($M_n = 28{,}619$), narrower PDI (1.2), and deeper $E_{HOMO} = -5.33$ eV. The deeper E_{HOMO} is important to have higher open-circuit voltage for the BHJ solar-cell.[15] Later on the solar cell device based on P1 : C_{60} (1 : 1) blend showed 128 mV higher V_{oc} (0.808 V for our P1) and P1 : $PC_{60}BM$ (1 : 2) showed 121 mV higher V_{oc} (0.801 V for our P1) compared to the previously reported (0.68 V or 680 mV) for a similar polymer LaPPs45 : C_{60} blend.

We have further synthesized (same reaction conditions) another polymer *poly*[(1,4-bis(dodecyloxy)benzene-2,5-diyl)-*alt*-(2,2′:5′,2″-terthiophene-5,5″-diyl)] (P2) with good molecular weight ($M_n = 18{,}660$), and narrow PDI (1.1). For the second polymer P2, we have replaced the 9,9-didodecylfluorene unit with the *p*-dodecyloxybenzene. This replacement is based on an observation from the density functional theory (DFT) computation results, which suggests that oxygen (O) of the alkoxy group and sulphur (S) from the thiophene units if close enough then they can have S···O noncovalent intermolecular interactions.[16] These interactions could help the macromolecule to achieve more planar structure. If this happens, then we should observe more red-shifted absorption. Later experimental observations (UV–vis spectra) and DFT calculations confirmed our expectation.

In this report, we present two polymers P1 and P2 synthesized via Stille cross-coupling reaction and well characterized by the gel permeation chromatography (GPC), nuclear magnetic resonance (NMR), Fourier transform infrared (FTIR), UV–vis, thermogravimetric analysis (TGA) and cyclic voltammetry (CV) analysis. We have studied their optoelectronic, thermal, V_{oc}, and solar cell properties blended with C_{60} and $PC_{60}BM$.

EXPERIMENTAL

Instruments and Materials

Proton and carbon (^{1}H and ^{13}C-NMR) NMR spectra were measured at 400 and 100 MHZ, respectively, on a Bruker Avance-400 spectrometer. UV–visible absorption spectra were recorded on a Shimadzu UV-2450 spectrophotometer. FT-IR spectra were obtained with Perkin–Elmer SP instrument. Elemental analyses were carried out on an LECO 932 CHNS elemental analyzer. The molecular weight of polymers was determined on a Waters 1525/2414 GPC, using tetrahydrofuran (THF) as the eluent at room temperature and polystyrene as the internal standard. TGA curves were measured with a PerkinElmer Pyris 1 instrument using 8 mg solid samples under nitrogen at a heating rate of 10°C/min. CV was done on a CHI600A electrochemical workstation with Pt disk coated by a polymer film, Pt plate, and standard calomel electrode (SCE) as working electrode, counter electrode, and reference electrode, respectively, in a 0.1 mol/L tetrabutylammonium hexafluorophosphate (Bu_4NPF_6) dissolved in pure (99.9%) anhydrous CH_3CN solution. The CV curves were recorded versus the potential of *SCE*, which was calibrated by the ferrocene/ferrocenium (Fc/Fc^+) redox couple (4.8 eV below the vacuum level). DFT calculations were performed on an Acer Computer. All reagents were obtained from Aldrich or Acros, Chemical Co. and used as received.

Synthesis of Monomers, Co*p*olymers P1 and P2

The 2,7-dibromo-9,9-didodecylfluorene[17] (DBRBDDF), 1,4-dibromo-2,5-bis(dodecyloxy)benzene[18] (DBRDDDOB) 2,2′:5′,2″-terthiophene (TERTH), and 5,5″-bis(trimethylstannyl)−2,2′:5′,2″-terthiophene[19] were synthesized according to the literature procedures and their NMR spectra (Figures S-1–S-7) are given in the Supporting Information. To synthesize the polymers P1 and P2, the purified monomers 2,7-dibromo-9,9-didodecylfluorene or 1,4-dibromo-2,5-bis(dodecyloxy)benzene were copolymerized with the 5,5″-bis(trimethylstannyl)−2,2′:5′,2″-terthiophene by the palladium-catalyzed, Stille cross-coupling reaction (Scheme 1) as described below in detail.

For both the polymers P1 and P2, 1 mmol of the different monomers were used. For P1, monomer 2,7-dibromo-9,9-didodecylfluorene (661 mg, 1 mmol), and for the P2, 1,4-dibromo-2,5-bis(dodecyloxy)-benzene (605 mg, 1 mmol) were added to a round-bottom flask fitted with reflux condenser (under nitrogen atmosphere) containing the monomer 5,5″-bis(trimethylstannyl)−2,2′:5′,2″-terthiophene (574 mg, 1 mmol). The catalysts $Pd_2(dba)_3$ (50 mg), $P(o\text{-}tolyl)_3$ (50 mg) and degassed anhydrous toluene (20 mL) were added and allowed to stir at room temperature for 15 min. The reaction mixture was then heated to reflux at 80°C under N_2 for 3 days. After this time, the reaction mixture was allowed to cool (room temperature) and poured into a conical flask containing 100 mL pure methanol (99.8%). The solid so obtained was subjected to further purification by Soxhlet extraction with diethyl ether, acetone, ethanol, and finally the polymeric material was extracted with pure and dry chloroform. To get better purification, the polymer in chloroform was passed through a thin glass column containing Bio-Beads (S-X1, 200–400 mesh, catalog#152–2150, benzene swelling 7.4 mL/g). The solvent was then removed under vacuum and dried by mild heating under vacuum and N_2 flow. The solids so obtained were characterized by the ^{1}H-NMR and other techniques (Supporting Information Figures S-8, S-9, and data). The two copolymers are processable due to their good solubility in organic solvents such as THF, $CHCl_3$, toluene, chlorobenzene and *o*-dichlorobenzene.

Photovoltaic Device Fabrication and Characterization

PSCs were fabricated with indium tin oxide (ITO) precleaned glass as the anode, Al as the cathode, and a blended film of

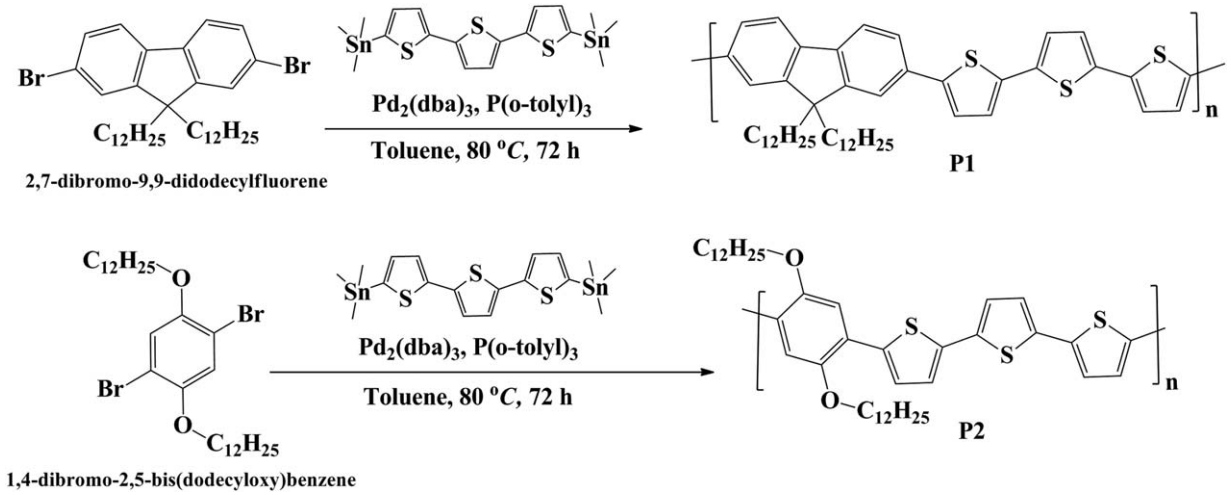

Scheme 1. Synthetic route to P1 and P2.

polymer : C_{60} as the photoactive layer. The PEDOT : PSS [*poly*(3,4-ethylenedioxythiophene) : *poly*(styrenesulfonate)] (Baytron P 4083, Germany) was spin-coated (30 nm thick) on the ITO substrate. Then, a 20 mg/mL solution of the polymer and C_{60} (1 : 1, w/w) in *Chloroform* ($CHCl_3$) pre-stirred overnight was spin-coated at 1000 rpm for 30 s onto the PEDOT : PSS layer. The thickness of the photoactive layer is about 60 nm (calibrated by an Ambios Technology XP-2 profilometer). At last, a 100-nm-thick Al film was deposited on the photoactive layer under vacuum of 4×10^{-4} Pa. The active area of PSCs is 9 mm^2. Current–voltage characteristics of the devices under illumination of a Thermal Oriel solar simulator with AM 1.5 solar irradiation (100 mW/cm^2) were recorded on a semiconductor parameter analyzer (Keithley 2400-SCS).

RESULTS AND DISCUSSION

Polymer Design, Synthesis, and Characterization

After polymerization followed by purification, if all the macromolecules in a sample could have the same chain length, then weight-average (M_w) and number-average molecular weight (M_n) values would be identical. However, due to the distribution of number of polymerized units in a real sample, the weight-average value can be higher than the number-average value. The ratio between M_w and M_n is called the polydispersity index (PDI = M_w/M_n). We determined the molecular weight distribution of the polymers by the size-exclusion chromatography (GPC, THF). As presented in Table I, the M_w, M_n, and PDI of the P1 [Supporting Information Figure S10(a)] are 28,619, 23,485 g mol^{-1}, and 1.21 respectively. Similarly for the P2, the corresponding M_w = 20,754 g mol^{-1} and M_n = 18,660 g mol^{-1} [Supporting Information Figure S10(b)], which gives PDI = 1.11. The molecular weights and PDIs show a polycondensation reaction and narrow molecular weight distribution of the macromolecules.[20] The polymer was further characterized by the ^{1}H-NMR.

The polymer P1 was obtained as a dark solid (523 mg, yield 70%). The ^{1}H-NMR (Supporting Information Figure S8) of the polymer P1 in $CDCl_3$ at room temperature showed the aromatic region (fluorene) as 2 pairs of peaks at 7.71–7.69 and 7.54–7.52 ppm attributed to the H_f (m, fluorene Ar-H) for the 6 aromatic hydrogens of fluorene. These peaks are similar to the pair of peaks at 7.52–7.50 and 7.45–7.43 ppm (6 Ar-Hs) in the aromatic region of the monomer 2,7-dibromo-9,9-didodecylfluorene (Supporting Information Figure S1). The broad peaks at 7.16–6.99 ppm attributed to the H_e (brm, Thiophene Ar-H), observed for the 6 aromatic hydrogens of the terthiophene unit in the polymer. These δ values are similar to the terthiophene which shows peaks between 7.23 and 7.01 ppm (Supporting Information Figure S5). In the aliphatic region, broad triplet was observed at 1.70–1.67 ppm attributed to the H_d. These are the 4 Alkyl-Hs (2 × CH_2) next to the C^9 of the fluorene (4H, FluoreneC^9-($\boldsymbol{CH_2}$)$_2$). The broad multiplet at 1.44–1.39 ppm is attributed to the H_c (brm, 4H, FluoreneC^9 (CH_2-$\boldsymbol{CH_2}$)$_2$). The taller multiplet at 1.31–1.07 ppm is attributed to the H_b (brm, 28H, 14 × CH_2) and the last multiplet (combination of triplet and multiplet) at 0.93–0.88 ppm is attributed to the terminal 14 Alkyl-Hs (m, 14H, 2×($CH_3(CH_2)_2$)$_2$).

The polymer P2 was obtained as a dark solid (458 mg, yield 66%). The ^{1}H-NMR (Supporting Information Figure S9) of the polymer P2 in the solvent $CDCl_3$ at room temperature showed the aromatic region (e, didodecyloxybenzene and terthiophene) as four kinds of peaks at 7.48 (brs, 1Ar-H), 7.18 (m, 2Ar-H), 7.15–7.13 (brs, 1Ar-H), and 7.09 (m, 4Ar-H) for the 8 ArHs. The broad triplet at 4.15–4.12 ppm is attributed to the H_d (brt, Ar-(O-$\boldsymbol{CH_2}$-R)$_2$, 4H). The next broad multiplet at 1.97–1.93 ppm is attributed to the H_c (Ar-(OCH_2.$\boldsymbol{CH_2}$-R)$_2$, 4H). The multiplet at 1.25 ppm is attributed to the H_b (18xCH_2, 36H). The triplet at 0.88–0.84 ppm arises due to the terminal methyl

Table I. Molecular Weight Comparison Between P1 and P2

Polymer	M_w	M_n	PDI
P1	28,619[a]	23,485[a]	1.21[a]
P2	20,754[a]	18,660[a]	1.11

[a] Data from GPC (THF).

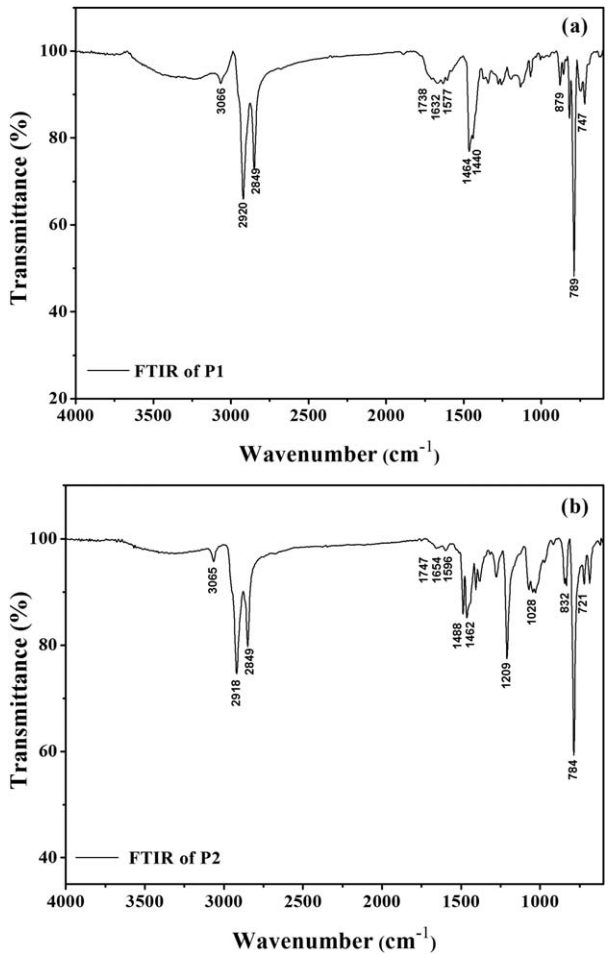

Figure 1. FTIR spectra (ATR) of the polymers (a) P1 and (b) P2.

groups attributed to the H_a (brt, 2xCH_3, 6H). The polymers P1 and P2 were further characterized by the FTIR spectroscopy.

FTIR analysis[21] (Figure 1, Table II) indicates that the aromatic hydrogen str. (=C—H) appears at 3067 cm^{-1} for the 2,2′:5′,2″-terthiophene (TERTH, Supporting Information Figure S13) 3066 cm^{-1} for the P1, and 3065 cm^{-1} for the P2. The 2,7-dibromo-9,9-didodecylfluorene (DBRBDDF, Supporting Information Figure S11) shows aliphatic C—H stretches at 2955, 2918, 2847 cm^{-1}. Similarly, the P1 shows aliphatic C—H stretches at 2920, 2849 cm^{-1}. The 1,4-dibromo-2,5-bis(dodecyloxy)benzene (DBRDDDOB, Supporting Information Figure S12) shows aliphatic —CH stretch at 2956, 2917, 2846 cm^{-1}. The P2 shows similar aliphatic —CH stretch at 2918, 2849 cm^{-1}. Similar to the monomer TERTH (Table II), the vibrations observed at 1741, 1648 cm^{-1} for the P1 and 1747, 1654 cm^{-1} for the P2 can be attributed to the terthiophene units (C=C str.) inside the main chain of the polymer. Mixed C=C vibrations (C=C str. of benzene and C=C str. of thiophene) were observed at 1577, 1464, 1440 cm^{-1} for the P1 and 1596, 1488, 1462 cm^{-1} for the P2. The DBRDDDOB shows 2 absorption peaks at 1208 and 1020 cm^{-1} for the RCH_2O-Ar (Ar.C-O str.) and RCH_2-OAr (Aliphatic C—O str.) respectively. Similarly, the polymer P2 shows two absorption peaks at 1209 (Ar.C—O str.) and 1028 cm^{-1} (Aliphatic C—O str.). Similar to the monomers, C—H Out of plane (*oop*) bending vibrations were observed for the P1 at 879, 789, 748 cm^{-1} and for the P2 at 832, 784, 721 cm^{-1}.

Optical Properties & DFT Calculations

The UV–vis spectra of these polymers showed that the D–D units of P1 and P2 are capable of decreasing the band gap. The UV–vis absorption spectra of the P1 [Figure 2(a)] and P2 [Figure 2(b)] in $CHCl_3$ dilute solution (1×10^{-5} mol/L) and film (on quartz) were measured and the data is summarized in Table III. Similar to the π–π^* transition (446 nm in $CHCl_3$) of the *rr*-P3HT,[22] the UV–vis absorption ($CHCl_3$) showed π–π^* transitions as a broad band at 470 nm for P1 and 476 nm for P2. It is well known that the thin film of the *rr*-P3HT shows red-shifted peaks (vibronic structure), due to the π–π^* transitions, dimensional order, and intermolecular packing (via π-stacking) of the polymer chains in the solid state.[22,23] A more closely related UV–vis spectrum for the polymer LaPPS45 film has been studied in detail by the semi-empirical ZINDO/S simulation.[13] The polymer LaPPS45 film showed main peaks at 470,

Table II. FTIR Peaks Assignments for the Monomers and the Polymers P1 and P2

Functional group	TERTH[a] (cm^{-1})	DBRBDDF[b] (cm^{-1})	P1[c] (cm^{-1})	DBRDDDOB[d] (cm^{-1})	P2[e] (cm^{-1})
=C—H (arom. Str.)	3067	–	3066	–	3065
Aliphatic —CH str.	–	2955, 2918, 2847	2920, 2849	2956, 2917, 2846	2918, 2849
C=C (str.,thiophene)	1742, 1645	–	1738, 1632	–	1747, 1654
C=C str.	1516, 1461, 1422	1597, 1571, 1450	1577, 1464, 1440	1492, 1458	1596, 1488, 1462
RCH_2O-Ar	–	–	–	1208	1209
RCH_2-OAr	–	–	–	1020	1028
C—H *oop*	833, 801, 796	880, 814,753	879, 789, 747	849, 807, 764	832, 784, 721

[a] Data from Supporting Information Figure S13.
[b] Data from Supporting Information Figure S11.
[c] Data from Figure 1a.
[d] Data from Supporting Information Figure S12.
[e] Data from Figure 1b.

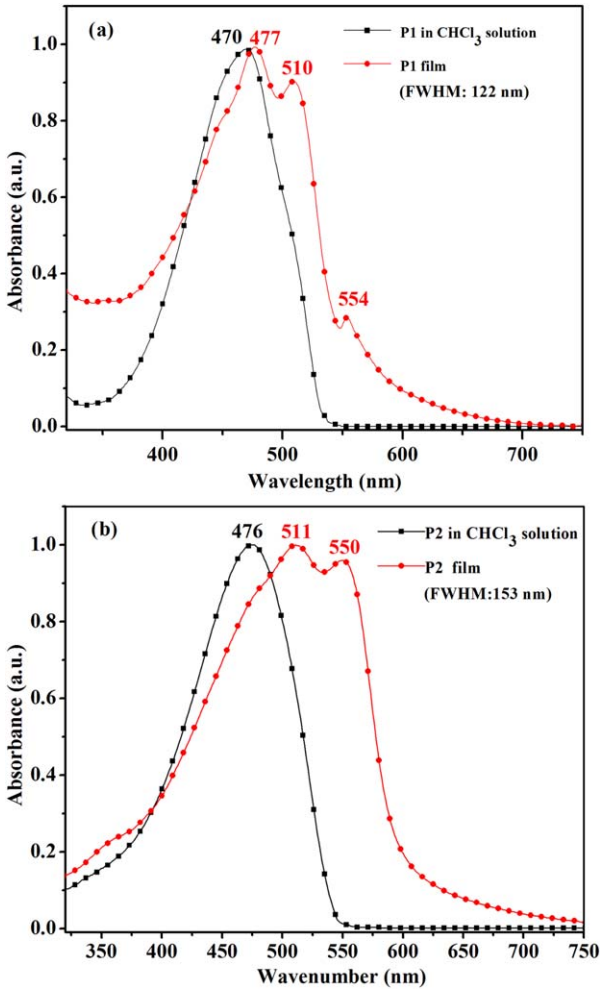

Figure 2. UV–vis absorption spectra of (a) P1 and (b) P2 in $CHCl_3$ solution and film (on Quartz). [Color figure can be viewed in the online issue, which is available at wileyonlinelibrary.com.]

500 and 541 nm. The peak at 470 nm was attributed to the π–π^* transition, 500 nm to the π-π^* transition and aggregation, and 541 nm only to the aggregation structure (π-stacking). Based on these observations, we can attribute the three red-shifted peaks at 477, 510, 554 nm (for the P1 film) and two peaks at 511, 550 nm (for the P2 film) in the UV–vis spectra [Figure 2(a,b)] to the π–π^* transitions and π-stacking in the solid state. The π-stacking is an important property of high-performance polymers for the solar cell application.[24] From the onset wavelengths of the thin films (λ_{onset}, Table III), we estimated ($E_g^{opt} = 1240/\lambda_{onset}$)[25] the optical band gaps (E_g^{opt}) to be 2.04 eV for the P1 and 2.00 eV for the P2. If we compare the UV–vis absorption spectra of P1 and P2, we can observe that the solution λ_{max}, film λ_{max}, and full width at half maximum (FWHM) of the P2 are higher than the P1, resulting in the lower band gap of P2. This happens due to the oxygen (O) of the alkoxy group and sulphur (S) from the neighbor thiophene units to have S···O interactions resulting in more planar macromolecular structure.[16]

To understand and explain the planarity problem of the P1 and P2, we performed the DFT calculations. The alkyl chain lengths were decreased to the methyl units and only dimers A (from P1) and B (from P2) (Figure 3) were subjected to the calculations due to the limitations of computational time and resources. The two molecular structures (A and B) were subjected to the Becke's three-parameter DFT in combination with the Lee–Yang–Parr's correlation functional (B3LYP) and 6–31G(d, p) basis sets[26,27] within the Wavefunction Spartan 08.[28]

The DFT output molecular structures and selected Mulliken Charges[29,30] are given in Figure 3 (Supporting Information Figure S14 shows structures and Mulliken Charges of all the atoms). It is well known that smaller the dihedral angle (φ, three dimensions are indicated by the curved blue and straight red arrows) between the combined units, higher is the planarity. We observed that $\varphi_2 = 16.03°$ for the unit B (P2) is much smaller than $\varphi_1 = 25.47°$ for the unit A (P1). Therefore, it is very likely that the P2 can show more planar structure as compared to the P1. The higher planarity (unit B) is likely caused by a partial negative charge (Mulliken Charge = −0.530) on the oxygen and partial positive charge on the nearest Sulfur (Mulliken Charge = +0.295) which is absent in the unit A. The more likely (due to opposite charges) space interaction between sulfur and nearest oxygen gives shorter space distance of 2.742 Å (S···O, unit B) as compared to the less likely (only positive charge) longer 2.783 Å between the S and the nearest H in the unit A.

Thermal Properties

From a solar cell perspective, the conjugated polymers should be thermally (annealing) stable especially between 100 and 200°C to enhance the solar cell efficiency.[31,32] Therefore, the thermal stability of the P1 and P2 was investigated by the TGA (Figure 4) under the nitrogen atmosphere to measure the T_d (onset decomposition temperature). Both the polymers P1 ($T_d = 418°C$) and P2 ($T_d = 365°C$) displayed good thermal stability.

Electrochemical Properties

Cyclic voltammetry (CV) was used to investigate the electrochemical properties of P1 and P2. The CVs were recorded (films on the working electrode, solvent CH_3CN, and electrolyte Bu_4NPF_6) at the fixed scan rate of 0.01 V/s as shown in Figure 5(a,b) (positive and negative scans) respectively and their electrochemical properties are summarized in the Table IV and Figure 6.

The CVs (positive scan) of the two polymers show that both the P1 and P2 are good electron donors (doping & dedoping) processes. The onset oxidation potential (vs *SCE*) E_{ox} for P1 is 0.93 V and 0.65 V for P2. From the oxidation potential values,

Table III. Optical Properties Comparison Between P1 and P2

Polymer	λ_{max} (sol, nm)	λ_{max} (film, nm)	λ_{onset} (film, nm)	E_g^{opt} (eV)
P1[a]	470[a]	477, 510, 554[a]	605[a]	2.04[a]
P2[b]	476[b]	511, 550[b]	617[b]	2.00[b]

[a] Data from Figure 2a.
[b] Data from Figure 2b.

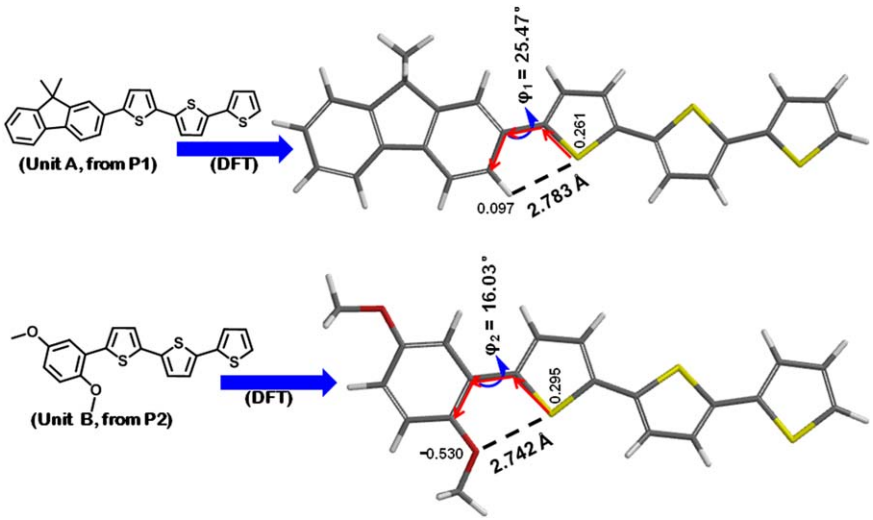

Figure 3. Output molecular structures of unit A (P1) and unit B (P2). [Color figure can be viewed in the online issue, which is available at wileyonlinelibrary.com.]

the HOMO energy levels (E_{HOMO}) of the two polymers can be estimated using the equation [$E_{HOMO} = -E_{ox} + 4.4$) eV].[33] The calculation gives HOMO energy level, E_{HOMO} for the P1 = −5.33 eV and −5.05 eV for the P2. These E_{HOMO} levels are deeper when compared to the *rr*-P3HT as previously reported (−4.8 eV by Boer *et al.*[34]). The deeper E_{HOMO} can help to enhance the V_{oc} of the polymer [$V_{oc} = E_{LUMO}$ (acceptor) − E_{HOMO} (donor) − 0.3 V].[35] The P1 showed, $E_{HOMO} = -5.33$ eV close to the ideal polymer whose $E_{HOMO} = -5.4$ eV.[36] Previously a donor–acceptor design strategy (D–A polymer) has been suggested to achieve the best possible E_{HOMO} level but in our case, a simple donor–donor (D–D polymer) design has shown to produce the similar results.[15] The CVs (negative scan) of the two polymers showed the reduction potential $E_{red} = -0.82$ V (vs *SCE*) for P1 and −0.80 V (vs *SCE*) for P2. From the reduction potential values, the LUMO energy levels (E_{LUMO}) of the two polymers can be estimated using the equation [$E_{LUMO} = -(E_{red} + 4.4)$ eV].[33] The calculation gives LUMO energy level, E_{LUMO} for the P1 = −3.58 eV, and −3.6 eV for the P2.

Figure 7 shows the energy levels $E_{HOMO} = -6.2$ eV and $E_{LUMO} = -4.3$ eV for the C_{60}.[37] The energy levels of the polymers P1 (donor) and P2 (donor), when combined with the energy level of the C_{60} (acceptor), can help us to estimate upper limit (pink solid horizontal line in Figure 6) of the calculated open circuit voltage ($^{UL}V_{oc} = E_{LUMO}$ (acceptor) − E_{HOMO} (donor), unit: V) of the solar cell.[37] The calculation gives $^{UL}V_{oc} = 1$ V for the P1 and 0.7 V for the P2. These calculations predict that the P1 should show higher V_{oc} as compared to the P2.

Photovoltaic Properties

To evaluate the photovoltaic property of the polymers P1 and P2, BHJ-PSCs were made with the device structure of ITO/PEDOT : PSS/Polymer : C_{60}(1 : 1, w/w)/Al. Figure 7 shows the *J–V* curves of the PSCs under the illumination of AM 1.5 solar irradiance (100 mW/cm^2), when the devices were tested through the glass/ITO side.

The PCE (η) of a solar cell device is given by $\eta = FF\ J_{sc}\ V_{oc}/P_{in}$, where V_{oc} is the open circuit voltage or voltage under open-circuit condition (V), J_{sc} is the short circuit current-density or photocurrent density under zero-bias (A/cm^2), *FF* is the fill factor (%), and P_{in} is the incident light power (W/cm^2). The fill factor is defined as the ratio of the largest output power (V_m J_m) to the product of V_{oc} and J_{sc}, i.e., $FF = V_{max}\ J_{max}/V_{oc}\ J_{sc}$, where V_{max} and J_{max} are the current density and the voltage at the maximum power point of the current–voltage (*J–V*) in the fourth quadrant.[38,39]

The solar cell data is summarized in the Table V. We observed that the PSC based on P1 : C_{60} = 1 : 1 blend showed PCE of 0.94% (annealed at 100°C), with a $V_{oc} = 0.808$ V, short circuit current density (J_{sc}) of 3.06 mA/cm^2, and fill factor (*FF*) of 38.05%. The PCE of P1 with C_{60} blend is lower than the

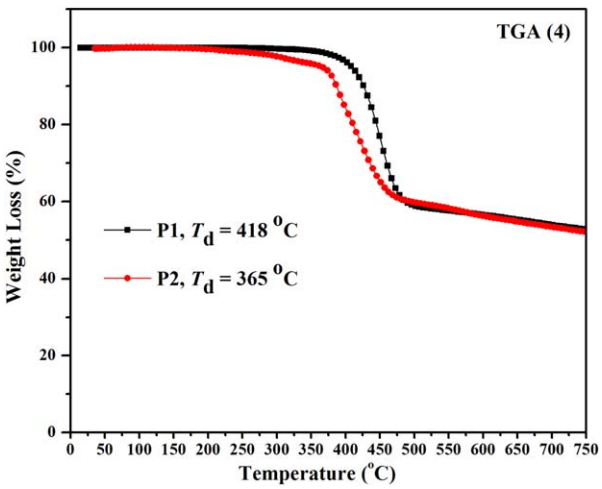

Figure 4. TGA curves of P1 and P2. [Color figure can be viewed in the online issue, which is available at wileyonlinelibrary.com.]

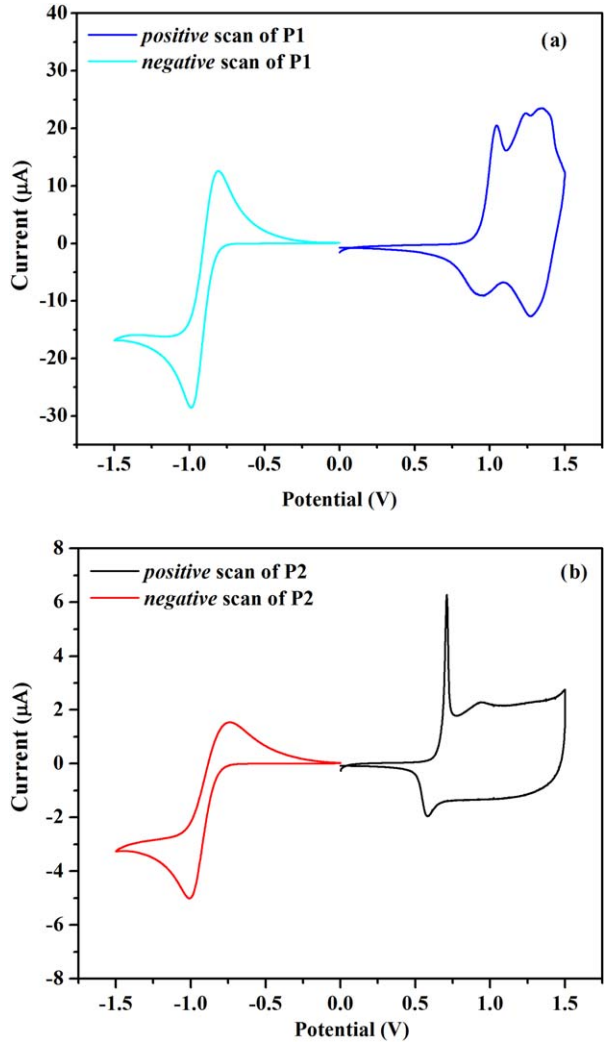

Figure 5. Cyclic voltammograms measured for polymer films (a) P1 and (b) P2 on a glassy carbon electrode in 0.1 mol/L Bu_4NPF_6 in CH_3CN as electrolyte solution. [Color figure can be viewed in the online issue, which is available at wileyonlinelibrary.com.]

polymer LaPPs45 but P1 showed 128 mV higher V_{oc} (0.808 V) as compared to the 0.68 V for the LaPPs45. This is due to the deeper E_{HOMO} of the P1 compared to the LaPPs45 as expected from the CV measurements, and calculated upper limit of the V_{oc}.

Similarly, the PSC based on P2 : C_{60} = 1 : 1 blend showed PCE of 0.71% (annealed at 100°C), with a V_{oc} = 0.720 V, short circuit current-density (J_{sc}) of 3.64 mA/cm^2, and fill factor (FF) of 27.17%. P1 displayed higher *FF* and V_{oc} resulting in better PCE of P1 when compared to the P2. This observation signifies the

Table IV. Electrochemical Results from Cyclic Voltammetry of Polymer Films

Polymer	E_{ox} (V)[a]/*HOMO* (eV)[b]	E_{red} (V)[a]/*LUMO* (eV)[b]	E_g^{ec} (eV)[c]
P1	0.93/−5.33	−0.82/−3.58	1.75
P2	0.65/−5.05	−0.80/−3.6	1.45

[a] *Onset*-peak potentials *vs. SCE*.
[b] Energy levels are estimated from $E_{HOMO/LUMO} = -(E_{ox/red} + 4.4)$ eV.
[c] Electrochemical band gap.

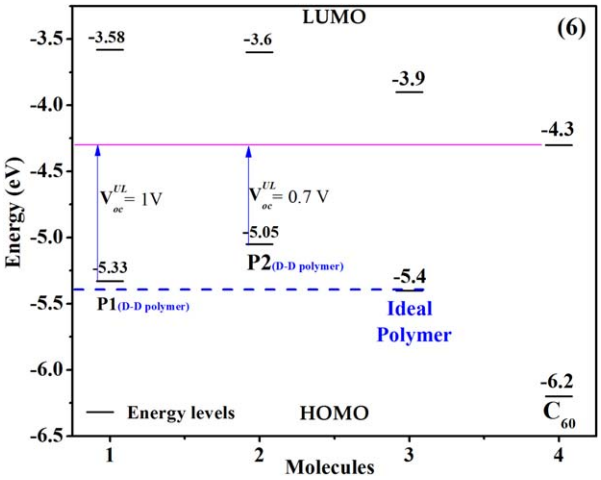

Figure 6. Energy level comparison for the polymers P1, P2, ideal polymer, and C_{60}. [Color figure can be viewed in the online issue, which is available at wileyonlinelibrary.com.]

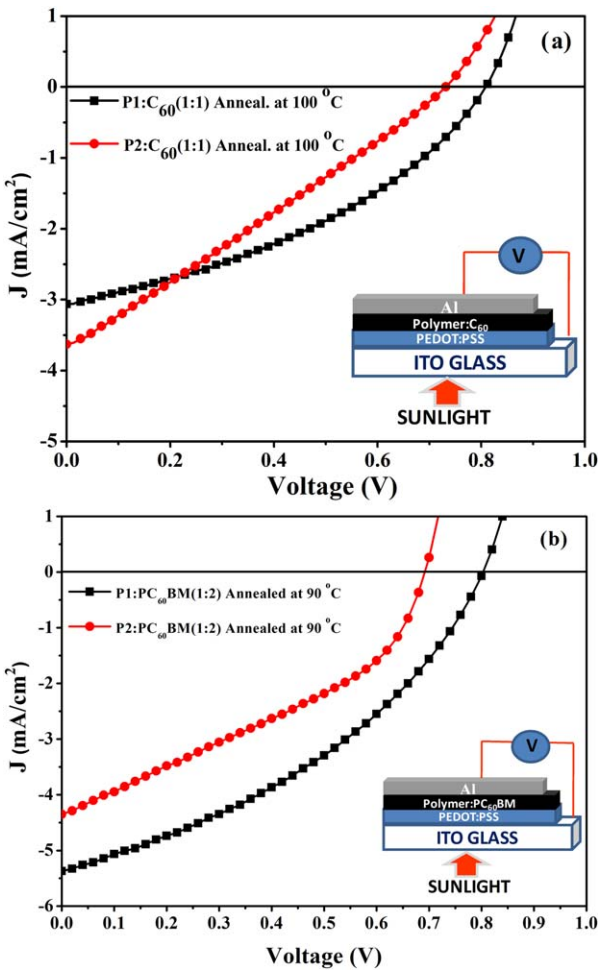

Figure 7. *J–V* curves for the solar cells made from (a) polymer : C_{60} and (b) polymer : $PC_{60}BM$. [Color figure can be viewed in the online issue, which is available at wileyonlinelibrary.com.]

Table V. Solar-Cell Parameter Comparison for the P1 and P2

Polymer : acceptor	Anneal. temp. (°C)	M_w (kDa, PDI)/ E_{HOMO} (eV)	Band gap (eV)	J_{SC} (mA/cm^2)	V_{oc} (mV)	FF (%)	η (%)	Data
P1 : C_{60} (1 : 1)	100	28.6(1.2)/−5.33	2.04	3.06	808.8	38.05	0.94[7a]	T.W.
PFTT	N.A.	4.72/−5.08	2.05	N.A.	N.A.	N.A.	N.A.	*Ref.* [12]
LaPPS45/C_{60}(bilayer)	70–200	N.A.	N.A.	6.80	680	50	2.33	*Ref.* [13]
LaPPS45 : C_{60}(1 : 1)	100	5.5(2.2)/−5.2	2.05	6.30	680	55	2.33	*Ref.* [14]
P2 : C_{60}(1 : 1)	100	20.7(1.1)/−5.05	2.00	3.63	720	27.17	0.71[7a]	T.W.
PBTB(OC_7H_{15})$_2$: $PC_{60}BM$(1 : 4)	N.A.	6.34(1.3)/−5.4	2.1	2.49	740	32	0.59	*Ref.* [42]
PBTB($OC_{12}H_{25}$)$_2$: $PC_{60}BM$(1 : 4)	N.A.	3.95(1.3)/−5.5	2.1	1.59	760	39	0.48	*Ref.* [42]
JC-1 : $PC_{60}BM$ (1 : 1)	N.A.	11.7(2.4)/N.A.	2.22	2.6	560	29	0.4	*Ref.* [43]
P1 : $PC_{60}BM$ (1 : 2)	90	28.6(1.2)/−5.33	2.04	5.37	801.5	38.29	1.65[7b]	T.W.
P2 : $PC_{60}BM$ (1 : 2)	90	20.7(1.1)/−5.05	2.00	4.34	691	36.45	1.09[7b]	T.W.

importance of fluorene. Although, the PCE of the P1 and P2 is not high, but can be improved by further research on other parameters like varying the C_{60} content, different annealing temperatures, use of additive, use of different processing solvents, use of acceptors such as the $PC_{60}BM$ or $PC_{70}BM$ and morphology of the active layer.[40]

There can be exceptions but higher molecular weight polymers are capable to improve PCE and stability but need more intensive investigation of the three variables V_{oc}, *FF*, and J_{sc} under constant P_{in} (AM1.5).[10,41] Therefore, we have compared[12–14,42,43] our solar cell data with the reported data for the similar polymer backbone (Table V, Figure 8). The comparison shows that our polymers show higher V_{oc} with lower FF and J_{sc} for P1[12–14] but Lower V_{oc}, higher FF and J_{sc} for the P2, responsible for the higher PCE (for P2) when compared to the previous reports.[42,43] These parameters are dependent upon optical absorption (HOMO-LUMO levels, film λ_{max}, and bandgap) of the composite, type of acceptor, polymer-to-acceptor ratio in the blend film, solvent processing, film growth methods (nano-size domain morphology), annealing temperature, and many others.[8,9,44]

To improve the PCE of P1 and P2, we applied the composite Polymer : $PC_{60}BM = 1 : 2$ (w/w in anhydrous pure (99.9%) $CHCl_3$, under N_2), and annealing at 90°C for 20 min with the

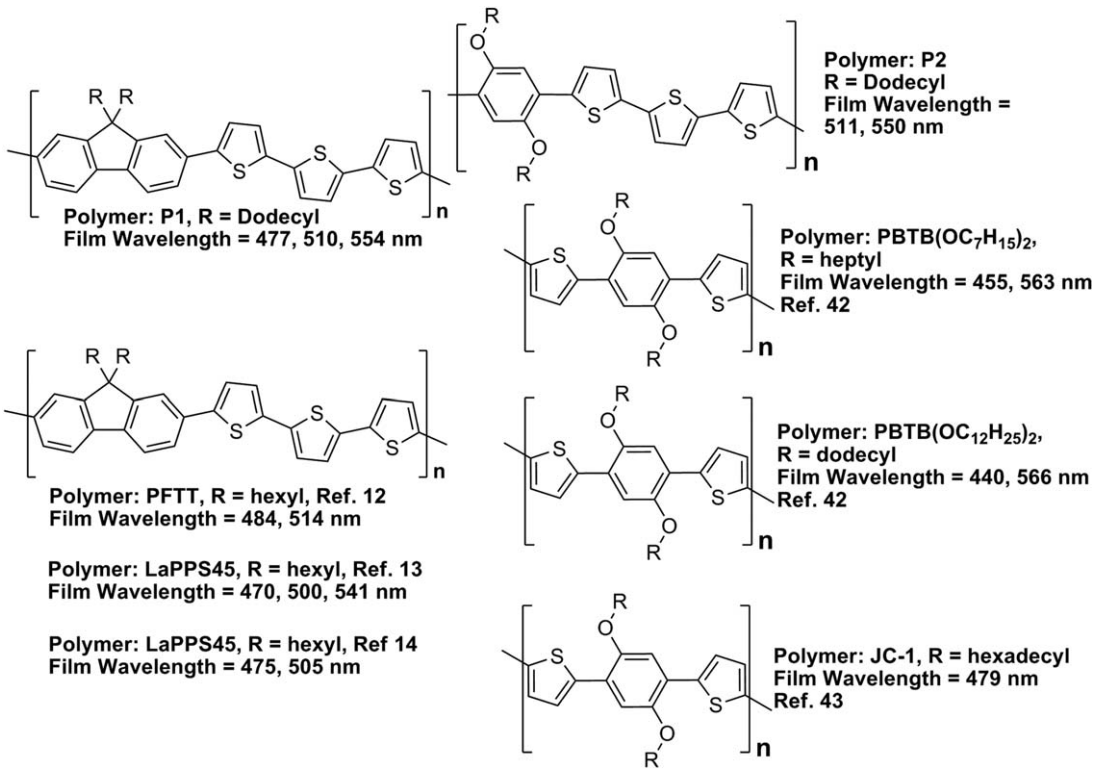

Figure 8. Polymers of Table V and their λ_{max} (film) values.

device structure of ITO/PEDOT : PSS/Polymer : $PC_{60}BM$(1 : 1, w/w)/Al.[45] Figure 7(b) shows the *J–V* curves of the PSCs under AM 1.5 solar irradiance (100 mW/cm^2) and data is summarized in Table V (entries 9 and 10). The comparison of the data shows that PCE of the P1 and P2 improved to a new level of 1.65 and 1.09%, respectively. This is mainly due to the improvement in the J_{sc} and *FF*. The PCE of P1 is still not high possibly due to longer alkyl side chains, different optical properties (Figure 8, Table V), and solid-state morphology.[46,47] This trend of decrease in overall PCE is also observed (entries 6, 7, and 8, Table V) by the polymers $PBTB(OC_7H_{15})_2$, $PBTB(OC_{12}H_{25})_2$, and JC-1. The P1 displayed higher *FF*, J_{sc}, and V_{oc} resulting in better PCE of the P1 compared to the P2. A part from overall PCE, we would like to mention that P1 has simpler synthesis, close to the ideal polymer HOMO–LUMO levels (without any acceptor units), higher molecular weights, higher thermal stability, well-defined UV–vis, band gap, and higher V_{oc} (121–128 mV). These interesting properties are highly desirable as a donor component for the regular as well as for the tandem solar cells, where a relative high bandgap and high V_{oc} is necessary for the front sub-cell.[48] Therefore, we can expect better results in the future.

CONCLUSION

Two alternating conjugated polymers P1 and P2 were synthesized via Stille cross-coupling reaction and characterized by the GPC, NMR, FTIR, UV–vis, TGA, and CV analyses. The solution λ_{max}, film λ_{max}, and FWHM of the P2 are higher than the P1, resulting in the lower band gap of P2 (2.00 eV vs 2.04 eV for P1 eV) indicating more planar macromolecular structure likely caused by the S···O interactions in P2. The DFT showed that more likely (due to opposite charges) space interaction between sulfur and nearest oxygen gives shorter space distance of 2.742 Å (S···O, unit B) as compared to the less likely (only positive charge) longer 2.783Å between the S and the nearest H in the unit A. The P1 possessed lower HOMO energy levels closer to the ideal polymer without any acceptor units in the main-chain (backbone) which is a rare and an important property for a D–D polymer required for the higher V_{oc}.[13,29] Onset decomposition temperature (T_d) of the polymers showed good thermal stabilities (418°C for P1 and, 365°C for P2). Preliminary photovoltaic study disclosed that the PSC based on P1 : C_{60} (1 : 1) and P2 : C_{60} (1 : 1) blend showed a PCE of 0.94% (V_{oc} = 0.808 V, J_{sc} = 3.06 mA/cm^2, *FF* = 38.05%) and 0.71% (V_{oc} = 0.720 V, J_{sc} = 3.64 mA/cm^2, *FF* = 27.17%), respectively, under AM 1.5 illumination (100 mW/cm^2). The Polymer : $PC_{60}BM$ (1 : 2 w/w), increased the J_{sc}, *FF* and improved the PCE of P1 (1.65%) and P2 (1.09%). The P1 displayed higher *FF*, J_{sc}, and V_{oc} resulting in better PCE of the P1 compared to the P2, which signifies the importance of fluorene. Polymer P1 has simpler synthesis, close to the ideal polymer HOMO–LUMO levels, good molecular weights, good thermal stability, well-defined UV–vis, and bandgap. These good properties are important for the regular as well as for the tandem solar cells.

ACKNOWLEDGMENTS

This work is supported by the National Natural Science Foundation of China (Grant No. 21374044), the Major Special Projects of Jiangxi Provincial Department of Science and Technology (Grant No. 20114ABF05100), the Technology Plan Landing Project of Jiangxi Provincial Department of Education, and the JXNU Chemistry and Chemical Engineering Department (Personal Grant No. 004824). We highly appreciate the help of Prof. Dr. Yiwang Chen, Zhang Yong (Nanchang University) regarding the solar cell devices.

REFERENCES

1. Chen, H. Y.; Hou, J. H.; Zhang, S. Q.; Liang, Y. Y.; Yang, G. W.; Yu, L. P.; Yang, Y.; Wu, Y.; Li, G. *Nat. Photon* **2009**, *3*, 649.
2. Hains, A. W.; Liang, Z. Q.; Woodhouse, M. A.; Gregg, B. A. *Chem. Rev.* **2010**, *110*, 6689.
3. Sundarrajan, S.; Murugan, R.; Nair, A. S.; Ramakrishna, S. *Mater. Lett.* **2010**, *64*, 2369.
4. Zhou, H. X.; Yang, L. Q.; Stuart, A. C.; Price, S. C.; Liu, S. B.; You, W. *Angew. Chem. Int. Ed.* **2011**, *50*, 2995.
5. Hu, X. L.; Shi, M. M.; Chen, J.; Zuo, L. J.; Fu, L.; Chen, H. Z. *Macromol. Rapid. Commun.* **2011**, *32*, 506.
6. Liang, Y.; Yu, L. *Acc. Chem. Res.* **2010**, *43*, 1227.
7. Hu, X. L.; Fu, W. F.; Zuo, L. J.; Shi, H. Q.; Chen, M. R.; Liu, S. Y.; Pan, J. Y.; Fu, L.; Shi, M. M.; Chen, H. Z. *Tetrahedron* **2013**, *69*, 3419.
8. Li, Y. F. *Acc. Chem. Res.* **2012**, *45*, 723.
9. Thompson, B. C.; Frechet, J. M. *J. Angew. Chem. Int. Ed.* **2008**, *47*, 58.
10. Schilinsky, P.; Asawapirom, U.; Scherf, U.; Biele, M.; Brabec, C. *J. Chem. Mater.* **2005**, *17*, 2175.
11. Imin, P.; Cheng, F.; Adronov, A. *Polym. Chem.* **2011**, *2*, 411.
12. Lee, W. Y.; Cheng, K. F.; Wang, T. F.; Chueh, C. C.; Chen, W. C.; Tuan, C. S.; Lin, J. L. *Macromol. Chem. Phys.* **2007**, *208*, 1919.
13. Marchiori, C. F.; Yamamoto, N. A.; Grova, I. R.; Macedo, A. G.; Paulus, M.; Sternemann, C.; Huotari, S.; Akcelrud, L.; Roman, L. S.; Koehler, M. *Org. Electr.* **2012**, *13*, 2716.
14. Grova, I. R.; Macedo, A. G.; Roman, L. S.; Akcelrud, L. *Eur. Polym. J.* **2013**, *49*, 3539.
15. Huo, L.; Hou, J.; Zhang, S.; Chen, H. Y.; Yang, Y. *Angew. Chem. Int. Ed.* **2010**, *49*, 1500.
16. Lee, W.; Choi, H.; Hwang, S.; Kim, J. Y.; Woo, H. Y. *Chem. A: Eur. J.* **2012**, *18*, 2551.
17. Yang, N. C.; Park, Y. H.; Suh, D. H. *J. Polym. Sci. Part A: Polym. Chem.* **2003**, *41*, 674.
18. Khatyr, A.; Ziessel, R. *J. Org. Chem.* **2000**, *65*, 3126.
19. Asawapirom, U.; Guntner, R.; Forster, M.; Farrell, T.; Scherf, U. *Synthesis* **2002**, *9*, 1136.
20. Kanki, K.; Masuda, T. *Macromolecules* **2003**, *36*, 1500.
21. Pavia, D. L.; Lampman, G. M.; Kriz, G. S.; and Vyvyan, J. R. Infrared spectroscopy, in Introduction to Spectroscopy: A Guide for Students of Organic Chemistry, 4th ed.; Brooks/Cole, Cengage Learning: Belmont, CA, USA, **2009**.

22. Herrmann, D.; Niesar, S.; Scharsich, C.; Koühler, A.; Stutzmann, M.; Riedle, E. *J. Am. Chem. Soc.* **2011**, *133*, 18220.
23. Brown, P. J.; Thomas, D. S.; Kohler, A.; Wilson, J. S.; Kim, J. S.; Ramsdale, C. M.; Sirringhaus, H.; Friend, R. H. *Phys. Rev. B* **2003**, *67*, 064203.
24. Li, K.; Li, Z.; Feng, K.; Xu, X.; Wang, L.; Peng, Q. *J. Am. Chem. Soc.* **2013**, *135*, 13549.
25. Cao, J.; Zhang, W.; Xiao, Z.; Liao, L.; Zhu, W.; Zuo, Q.; Ding, L. *Macromolecules* **2012**, *45*, 1710.
26. Becke, A. D. *J. Chem. Phys.* **1998**, *98*, 5648.
27. Lee, C. T.; Yang, W. T.; Parr, R. G. *Phys. Rev. B: Condens. Matter. Mater. Phys.* **1988**, *37*, 785.
28. Yamada, H.; Matsuzaki, Y.; Higashii, T.; Kazama, S. *J. Phys. Chem. A* **2011**, *115*, 3079.
29. Mulliken, R. S. *J. Chem. Phys.* **1955**, *23*, 1833.
30. Astrand, P.-O.; Ruud, K.; Mikkelsen, K. V.; Helgaker, T. *J. Phys. Chem. A* **1998**, *102*, 7686.
31. Wang, T.-L.; Yang, C.-H.; Shieh, Y.-T.; Yeh, A.-C.; Chen, C.-H.; Ho, T.-H. *Mater. Chem. Phys.* **2012**, *132*, 131.
32. Pearson, A. J.; Wang, T.; Jones, R. A. L.; Lidzey, D. G. *Macromolecules* **2012**, *45*, 1499.
33. Wei, Y. F.; Zhang, Q.; Jiang, Y.; Yu, J. S. *Macromol. Chem. Phys.* **2009**, *210*, 769.
34. Asadi, K.; Gholamrezais, F.; Smiths, E. C. P.; Blom, P. W. M.; Boer, B. D. *J. Mater. Chem.* **2007**, *17*, 1947.
35. Scharber, M. C.; Mühlbacher, D.; Koppe, M.; Denk, P.; Waldauf, C.; Heeger, A. J.; Brabec, C. *J. Adv. Mater.* **2006**, *18*, 789.
36. Zhou, H.; Yang, L.; Stoneking, S.; You, W. *Appl. Mater. Interfaces* **2010**, *2*, 1377.
37. Opitz, A.; Bronner, M.; Brütting, W. *Appl. Phys. Lett.* **2007**, *90*, 212112.
38. Kymakis, E.; Alexandrou, I.; Amaratunga, G. A. J. *J. Appl. Phys.* **2003**, *93*, 1764.
39. Li, Z.; Zhao, X.; Lu, X.; Gao, Z.; Mi, B.; Huang, W. *Sci. China Chem.* **2012**, *55*, 553.
40. Chen, W.; Nikiforov, M. P.; Darling, S. B. *Energy Environ. Sci.* **2012**, *5*, 8045.
41. Liu, C.; Wang, K.; Hu, X. W.; Yang, Y. L.; Hsu, C.-H.; Zhang, W.; Xiao, S.; Gong, X.; Cao, Y. *ACS Appl. Mater. Interfaces* **2013**, *5*, 12163.
42. Kim, Y. G.; Galand, E. M.; Thompson, B. C.; Walker, J.; Fossey, S. A.; Mccarley, T. D.; Abboud, K. A.; Reynolds, J. R. *J. Macromol. Sci. A: Pure Appl. Chem.* **2007**, *44*, 665.
43. Carle, J. E.; Andreasen, J. W.; Jorgensen, M. *Sol. Energy Mater. Sol. Cells* **2007**, *91*, 379.
44. Yip, H. L.; Jen, A. K. Y. *Energy Environ. Sci.* **2012**, *5*, 5994.
45. Zhuang, W. L.; Zhen, H. Y.; Kroon, R.; Tang, Z.; Hellström, S.; Hou, L. T.; Wang, E.; Gedefaw, D.; Inganäs, O.; Zhang, F. L.; Andersson, M. R. *J. Mater. Chem. A* **2013**, *1*, 13422.
46. Al-Ibrahim, M.; Roth, H. K.; Schroedner, M.; Konkin, A.; Zhokhavets, U.; Gobsch, G.; Scharff, P.; Sensfuss, S. *Org. Electr.* **2005**, *6*, 65.
47. Prosa, T. J.; Winokur, M. J. *Macromolecules* **1996**, *29*, 3654.
48. You, J. B.; Dou, L. T.; Yoshimura, K.; Kato, T.; Ohya, K.; Moriarty, T.; Emery, K.; Chen, C.-C.; Gao, J.; Li, G.; Yang, Y. *Nat. Commun.* **2013**, *4*, 1446.